Geometric preconditioner for indirect shooting and application to hybrid vehicle

Olivier Cots, Rémy Dutto, Sophie Jan, Serge Laporte

Geometric preconditioner for indirect shooting and application to hybrid vehicle

Olivier Cots* Rémy Dutto†‡§ Sophie Jan‡ Serge Laporte‡

February 22, 2024

Abstract

In this article, we are interested in the hybrid electric vehicle torque split and gear shift problem, which can be formulated as a classical Lagrange optimal control problem with fixed initial condition. The Pontryagin's maximum principle gives necessary optimality conditions adjoining to the state a covector called costate. Thus, the optimal state trajectory has to be found among the projections of the lifted trajectories, called Pontryagin extremals, given by the maximum principle. The indirect simple shooting method aims to compute Pontryagin extremals reducing the resolution to the research of the initial costate. Classically, a Newton-like solver is used to compute zeros of the so-called shooting equations. The main drawback of this method is its sensitivity to the initial guess. Therefore, a good initial guess need to be given to make the Newton solver converge, which is not an easy task in practice. We propose a preconditioning method of the shooting function based on a geometrical interpretation of the costate, in relation with the reachable set of the extended system and the underlying symplectic structure. We numerically show that this method reduces the number of iterations of our solver. Remarkably, in our experiments, it is better to use the preconditioner than to provide an approximation of the costate solution.

Keywords. Pontryagin's maximum principle, Indirect shooting, Geometric preconditioner, Mathieu transformation, Costate interpretation, Hybrid electric vehicle.

1 Introduction

In this article, we consider the Hybrid Electric Vehicle (HEV) torque split and gear shift problem, where the goal is to determine the optimal torque split between the Internal Combustion Engine (ICE) and the Electric Motor (EM) which minimizes the fuel consumption, the initial and final State Of Charge (SOC) of the battery being fixed. The industrial model is given by Vitesco Technologies. This model requires data as the requested torque at each time: for the experiments, we consider the Worldwide harmonized Light vehicles Test Cycle (WLTC), which is one of the most used cycle for fuel consumption and pollutant emission evaluations. Motivated by a new method based on a bilevel decomposition of the optimal control problem and presented in [4], we consider only the first 100 seconds of the cycle.

This problem can be formulated as a classical Lagrange optimal control problem with simple limit conditions. The Pontryagin Maximum Principle (PMP) gives necessary optimality conditions lifting the optimal trajectory to the cotangent space and leads (under some hypotheses) to the resolution

*Institut de Recherche en Informatique de Toulouse, UMR CNRS 5505, Université de Toulouse, INP-ENSEEIHT, France.

†Vitesco Technologies, Toulouse, France.

‡Institut de Mathématiques de Toulouse, UMR CNRS 5219, Université de Toulouse, UPS, France.

§Corresponding author: remy.dutto@orange.fr.

of a Two-Point Boundary Value Problem (TPBVP). The most classical method to solve a boundary value problem is the indirect simple shooting, whose goal is to find a zero of the simple shooting function, the variable of the shooting function being the initial costate of the lifted trajectory. This resolution can be done with a Newton-like solver. We present in Figure 1 a state-control trajectory obtained by shooting for the problem we consider.

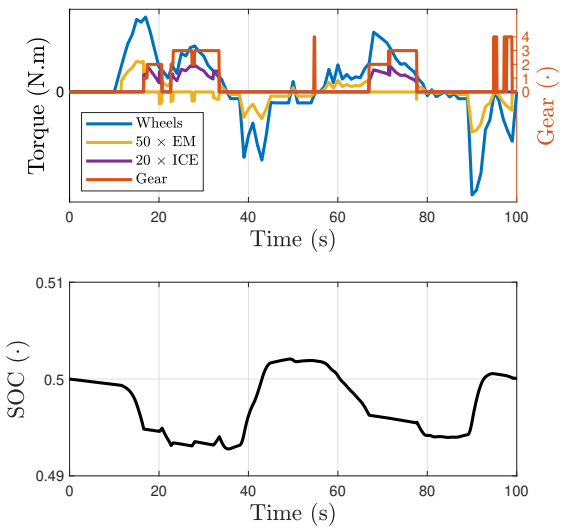

Figure 1: Optimal control (Gear and ICE torque) and state trajectory (SOC), with the initial and final state of charge fixed at 50%.

A drawback of the indirect simple shooting method is that a good initial guess needs to be provided to make the solver converge. This is not trivial in practice. To overcome this sensitivity issue, some methods have been developed such as indirect multiple shooting for instance (see [2]).

In this article, we propose a new method to reduce the sensitivity, and so to improve the convergence of the Newton-like solver. This method is a geometric preconditioner of the shooting function, and it is constructed using the Mathieu transformation applied to a change of variable of the extended state. This change of variable is constructed based on a geometrical interpretation of the costate and corresponds in our case to the affine transformation of an ellipse to a circle.

The article is organized as follows. The optimal control problem is formulated in Section 2. The Pontryagin Maximum Principle and the indirect simple shooting are recalled in Section 3. The construction of the proposed geometrical preconditioner of the shooting function is presented in Section 4, and the results are shown in Section 5. Section 6 concludes the article.

2 Optimal control problem

We consider the HEV torque split and gear shift problem described in details in [4]. This problem can be written into the following Lagrange Optimal Control Problem:

$$
\text{(OCP)} \qquad \begin{cases} \min\limits_{x,u} \displaystyle\int_{t_0}^{t_f} f^0\big(t, x(t), u(t)\big)\ \mathrm{d}t, \\ \text{s.t. } \dot{x}(t) = f\big(t, x(t), u(t)\big) & t \in [t_0, t_f] \text{ a.e.}, \\ \quad u(t) \in \mathrm{U}(t), & t \in [t_0, t_f], \\ \quad x(t_0) = x_0, \quad x(t_f) = x_f, \end{cases}
$$

where the goal is to find the optimal (absolutely continuous) SOC trajectory $x \in \mathrm{AC}([t_0, t_f], \mathbb{R})$ and the optimal (essentially bounded) control $u \in \mathrm{L}^\infty([t_0, t_f], \mathbb{R}^2)$. The control is composed of the gear and the torque split between ICE and the EM. The two functions f^0 and f, which respectively correspond to the instantaneous fuel consumption of the ICE and the SOC deviation, are supposed to be of class $\mathscr{C}^1$. The control domain $\mathrm{U}(t) \subset \mathbb{R}^m$ is a non-empty set for all $t \in [t_0, t_f]$ and corresponds to the physic limitations (discrete gear, ICE and EM rotation speed...). The initial x_0 and final x_f states are fixed, as well as the initial t_0 and final t_f times.

This optimal control problem is non-autonomous (due to the time dependency of the functions f^0 and f) because the requested wheel torque and rotation speed are obtained with the cycle (and some information of our HEV).

To transform the problem from Lagrange to Mayer form, we define the *extended state* $\tilde{x} = (x^0, x)$ where x^0 corresponds to the cost trajectory:

$$\dot{\tilde{x}}(t) = \tilde{f}\big(t, \tilde{x}(t), u(t)\big),$$

with $\tilde{f}(t, \tilde{x}, u) = \big(f^0(t, x, u), f(t, x, u)\big)$ the *extended system*. The initial extended state is set to $\tilde{x}_0 = (0, x_0)$. In order to recover the cost x^0 and the state x from an extended state $\tilde{x} = (x^0, x)$, we define the canonical x-space projection $\pi_x(\tilde{x}) = x$ and x^0-space projection $\pi_{x^0}(\tilde{x}) = x^0$. The final state condition becomes $\pi_x\big(\tilde{x}(t_f)\big) - x_f = 0$. From now on, we drop the $\tilde{}$ on variables to simplify the notations, keeping in mind that $x(t) \in \mathbb{R}^2$ stands for $\big(x^0(t), x(t)\big) \in \mathbb{R}^2$ and f for (f^0, f).

For any control law u, we define the mapping $u \mapsto x(u)$ as the solution at time t_f of the Cauchy problem

$$\dot{x}(t) = f\big(t, x(t), u(t)\big), \quad t \in [t_0, t_f] \text{ a.e.}, \quad x(t_0) = x_0.$$

This permits us to define the *admissible control set* $\mathcal{U}$ as the set of commands $u \in \mathrm{L}^\infty([t_0, t_f], \mathbb{R}^2)$ such that for all $t \in [t_0, t_f]$, $u(t) \in \mathrm{U}(t)$, and such that $x(u)$ is well defined. The *reachable set* is then given by $\mathcal{A} = x(\mathcal{U})$.

Figure 2 shows the reachable set $\mathcal{A}$ associated to (OCP). It is a non-empty closed convex set and we assume that $x_f \in \pi_x(\mathcal{A})$. In this frame, there exists a solution for Problem (OCP) and a necessary optimality condition for a pair (x, u) is that $x(t_f) \in \partial\mathcal{A}$, the boundary of $\mathcal{A}$.

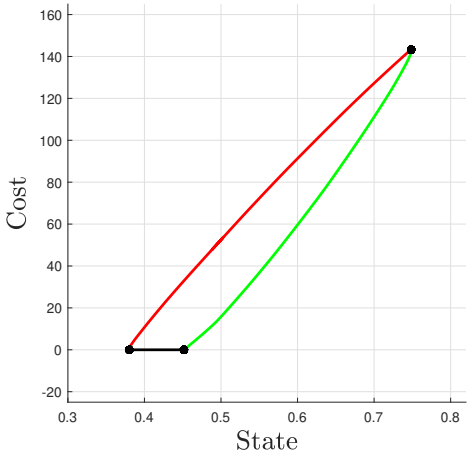

Figure 2: Reachable set $\mathcal{A}$ at time t_f, with $x_0 = (0, 0.5)$. The three black points correspond to corner points. The red (resp. green) line corresponds to $\partial\mathcal{A}$ when the cost is maximal (resp. minimal).

3 Necessary optimality conditions

3.1 Pontryagin Maximum Principle

According to the Pontryagin Maximum Principle (see [3, 6]), if the pair (x, u) is a solution of (OCP), then there exists a nontrivial *costate* trajectory $p \in \mathrm{AC}([t_0, t_f], \mathbb{R}^2)$, $\pi_{p^0}\big(p(t_0)\big) \leq 0$, such that the pair (x, p) with the control u, for almost every $t \in [t_0, t_f]$, follow the pseudo-Hamiltonian dynamics:

$$\begin{aligned} \dot{x}(t) &= \quad \nabla_p h\big(t, x(t), p(t), u(t)\big), \\ \dot{p}(t) &= -\nabla_x h\big(t, x(t), p(t), u(t)\big), \end{aligned} \tag{1}$$

and satisfy the maximization condition:

$$h\big(t, x(t), p(t), u(t)\big) = \max_{w \in \mathrm{U}(t)} h\big(t, x(t), p(t), w\big), \tag{2}$$

where $h(t, x, p, u) = \big(p \,\big|\, f(t, x, u)\big)$ is the *pseudo-Hamiltonian* and where for all $\tilde{p} = (p^0, p) \in \mathbb{R}^2$, $\pi_{p^0}(\tilde{p}) = p^0$ represents the p^0-space projection and $\pi_p(\tilde{p}) = p$ represents the p-space projection. We remark that the costate associated to the cost is constant since f does not depend on the cost. Hence, we can define $\pi_{p^0}(p) = \pi_{p^0}(p(t_0))$ for such a costate.

An *extremal* is defined as a couple (z, u), with $z = (x, p)$, such that the state $x \in \mathrm{AC}([t_0, t_f], \mathbb{R}^2)$, the costate $p \in \mathrm{AC}([t_0, t_f], \mathbb{R}^2)$ is not trivial and $\pi_{p^0}(p) \leq 0$, the command $u \in \mathrm{L}^\infty([t_0, t_f], \mathbb{R}^2)$ satisfies the constraint $u(t) \in \mathrm{U}(t)$ and such that (x, p, u) satisfies (1) and (2). A *BC-extremal* is an extremal that satisfies the boundary conditions $x(t_0) = x_0$ and $\pi_x\big(x(t_f)\big) = x_f$. Finally, an extremal is said to be *normal* if $\pi_{p^0}(p) < 0$ and *abnormal* if $\pi_{p^0}(p) = 0$.

For the sake of simplicity, we consider that for any extremal $(\bar{z}, \bar{u})$ the maximized pseudo-Hamiltonian provides a true *Hamiltonian*

$$H_t(z) = \max_{w \in \mathrm{U}(t)} h(t, x, p, w)$$

well defined and smooth (which means at least $\mathscr{C}^1$), for almost all $t \in [t_0, t_f]$ and for all z in a neighborhood of $\bar{z}(t)$. Under this assumption, the point (z, u) is an extremal of (OCP) if and only if $p \neq 0$, $\pi_{p^0}(p) \leq 0$ and for almost every $t \in [t_0, t_f]$

$$\dot{z}(t) = \vec{H}\big(t, z(t)\big),$$

where $H(t, z) = H_t(z)$ and $\vec{H}(t, z) = \big(\nabla_p H(t, z), -\nabla_x H(t, z)\big)$ is the *Hamiltonian vector field*.

3.2 Numerical methods

Under the previous assumption, that is in the Hamiltonian frame, the necessary optimality conditions given by the Pontryagin Maximum Principle lead to the resolution of the following Two-Point Boundary Value Problem:

$$\text{(TPBVP)} \qquad \begin{cases} \dot{z}(t) = \vec{H}\big(t, z(t)\big), \quad t \in [t_0, t_f] \text{ a.e.}, \\ x(t_0) = x_0, \quad \pi_x(x(t_f)) = x_f. \end{cases}$$

The classical numerical method to solve (TPBVP) is the indirect shooting method. The goal is to find a point where the shooting function $S \colon \mathbb{R}_- \times \mathbb{R} \to \mathbb{R}$ defined by

$$S(p) = \pi_x\big(\exp_{\vec{H}}(x_0, p)\big),$$

is equal to x_f, where we define $\pi_x(x, p) = \pi_x(x)$ and where $\exp_{\vec{H}}(z_0)$ corresponds to the solution at time t_f of the following Cauchy problem:

$$\dot{z}(t) = \vec{H}\big(t, z(t)\big), \quad t \in [t_0, t_f] \text{ a.e.} \quad z(t_0) = z_0.$$

Let us remark that the extremals are homogeneous in p: it can easily be shown that for all $k > 0$, if (x, p, u) is a BC-extremal of (OCP) then (x, kp, u) is also a BC-extremal of (OCP). Numerically, it is better to get rid of this homogeneity. There exist two main normalizations for this purpose:

- in the first normalization, the extremals associated to a solution of (OCP) are supposed to be normal ($p^0 < 0$). Under this assumption, we can fix $\pi_{p^0}(p) = -1$. The associated shooting function $S_p \colon \mathbb{R} \to \mathbb{R}$ is thus defined by

$$S_p(p) = S(-1, p).$$

- the second choice is to fix $||p||_2 = 1$. In this case, if we denote by α the angle of p, the associated shooting function $S_\alpha \colon [-\pi, 0] \to \mathbb{R}$ is therefore defined by

$$S_\alpha(\alpha) = S\big(\sin(\alpha), \cos(\alpha)\big).$$

The two corresponding shooting functions are shown in Figure 3.

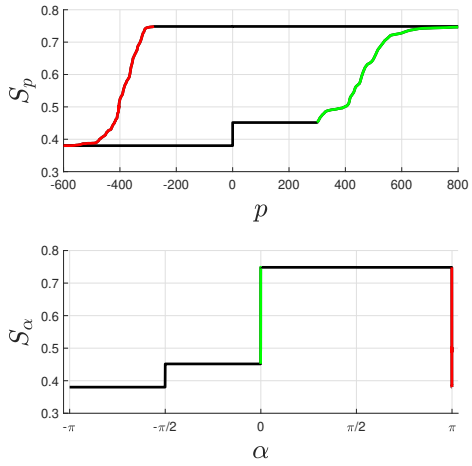

Figure 3: Shooting functions S_p and S_α. More precisely, in the upper figure, the green (with the bottom black) curve corresponds to the shooting function S_p and the red (with the upper black) one to the shooting function $S(1, p)$ (for which the goal would be to maximize the fuel consumption). In the same way, in the bottom figure, the shooting function corresponds to the restriction to the interval $[-\pi, 0]$.

For both normalizations, a zero of $S(\cdot) - x_f$ may be found using a classical Newton-like solver, which needs a good initial guess. Therefore, the bounds of the interesting part (the green one) of these shooting functions need to be determined. From Figure 3, we can notice that the range of interesting values (the green part) for S_α is extremely small.

4 Geometrical preconditioner of the shooting function

Paraphrasing Y. Saad, see [8, Chapter 9], preconditioning is simply a means of transforming the original system (not linear in our case) into one that is likely to be easier to solve with an iterative solver. Preconditioning aims to improve both efficiency and robustness of iterative techniques. The main goal of this article is thus to present a preconditioner that allows to reduce the sensitivity of the shooting function and permits to reduce the number of iterations of the Newton-like solver. This preconditioner is based on a geometric interpretation of the costate and the Mathieu transformation.

4.1 Geometric interpretation of the costate

The proof of the Pontryagin Maximum Principle is constructive, see [1] for instance. It is based upon the so-called needle variations introduced by Boltyanskii which generate a cone K_x, that can be seen as a local convex approximation of the set $\mathcal{A}$ at the point x. The extremals are then constructed by a backward integration of the Hamiltonian flow from (x, p), where p is taken in the non-empty polar cone K_x° of K_x. By construction, the cone K_x is included in the Bouligand tangent cone to $\mathcal{A}$ at x denoted $T(\mathcal{A}, x)$. Consequently, the normal cone to $\mathcal{A}$ at x, which is by definition the polar cone of $T(\mathcal{A}, x)$, is included in the cone K_x°, that is $N(\mathcal{A}, x) \subset K_x^\circ$. Hence, by construction, to any non-zero covector of $N(\mathcal{A}, x(t_f))$ is associated a BC-extremal. Let remark that since $\mathcal{A}$ is a non-empty close convex set, the normal cone $N(\mathcal{A}, x(t_f))$ is not reduced to $\{0\}$.

In Figure 4, the orientations of the final costates $p(t_f)$ are represented by the blue cones, anchored at the black, red and green points. It is easier now to understand the shape of the shooting function $S_\alpha(\cdot)$. Indeed, the normal cones associated to the corner points (in black) represent 99.84% of the angles while the interesting angles (associated to the green part) correspond only to 0.066%. In Figure 5 we give a neat representation of the relations between the angle of the covector and respectively the state and the cost at t_f.

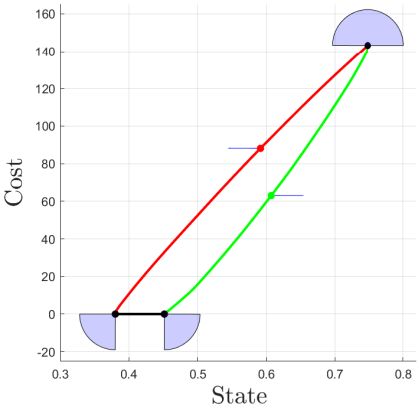

Figure 4: Similar to Figure 2. The blue cones correspond to the computed final costates orientations. Numerically, they happen to be the normal cones $N(\mathcal{A}, x(t_f))$ for different final states. Notice that the axes do not share the same scale and this explains why orthogonality is not obvious at first sight.

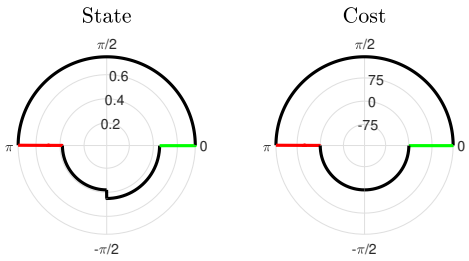

Figure 5: Final state (left) and cost (right) in a polar representation. The angle corresponds to α and the radius to the value of the state (left) and cost (right).

4.2 Symplectic manifold and Mathieu transformation

Let see $\mathbb{R}^2 = M$ as a smooth manifold. The cotangent bundle $T^*M \simeq \mathbb{R}^2 \times \mathbb{R}^2$ and the canonical symplectic form ω make a *symplectic manifold* (T^*M, ω). A Hamiltonian H is a smooth function defined on T^*M. If we denote by (x, p) the canonical Darboux coordinates on T^*M, the closed non-degenerate differential 2-form ω is obtained from the Liouville 1-form $\lambda = p\,\mathrm{d}x$ by $\omega = -\mathrm{d}\lambda = \mathrm{d}x \wedge \mathrm{d}p$. In other words, for all $u, v \in T_z(T^*M) \simeq \mathbb{R}^2 \times \mathbb{R}^2$, we have

$$\omega(u, v) = \big(u \,\big|\, Jv\big), \quad \text{where } J = \begin{pmatrix} 0 & I_{\mathbb{R}^2} \\ -I_{\mathbb{R}^2} & 0 \end{pmatrix}$$

is the classical symplectic matrix. The Hamiltonian vector field $\vec{H}$ is defined by $\omega(\vec{H}, \cdot) = \mathrm{d}H$, which leads to the Hamiltonian dynamics $\vec{H} = J\nabla H$.

We are now interested in transformations that preserve the symplectic form, and hence also the Hamiltonian dynamics. These transformations are called *symplectomorphisms* and correspond to the set of diffeomorphisms $\Phi\colon T^*M \to T^*M$ such that $\Phi^*\omega = \omega$. In particular, a diffeomorphism $\phi\colon M \to M$ is lifted into a symplectomorphism by the so-called Mathieu transformation

$$\Phi(x, p) = \big(\phi(x), J_\phi^{-\top}(x)\, p\big), \tag{3}$$

where $J_\phi(x)$ is the Jacobian matrix of ϕ at x and $J_\phi^{-\top}(x)$ denotes the transpose of its inverse. For more details about symplectic manifolds and the Mathieu transformation, we refer to [1] or [7].

4.3 Preconditioner construction

Let us consider a diffeomorphism $\phi\colon \mathbb{R}^2 \to \mathbb{R}^2$. The associated symplectomorphism Φ defined by (3) transforms $z = (x, p)$ into $w = (y, q)$:

$$z = \begin{pmatrix} x \\ p \end{pmatrix} \underset{\Phi^{-1}}{\overset{\Phi}{\rightleftarrows}} \begin{pmatrix} y \\ q \end{pmatrix} = w.$$

The relations between these variables is thus:

$$\begin{aligned} y &= \phi(x), & q &= J_\phi^{-\top}(x)\, p, \\ x &= \phi^{-1}(y), & p &= J_\phi^{\top}(x)\, q. \end{aligned}$$

The main idea is to create the shooting function $\bar{S}\colon \mathbb{R}^2 \to \mathbb{R}$ that takes the new system of coordinates q as input and returns the state in the original one:

$$\bar{S}(q) = S\big(J_\phi^{\top}(x) q\big).$$

In the same way as presented in Section 3.2, the homogeneity is removed by considering the two following shooting functions $S_q\colon \mathbb{R} \to \mathbb{R}$ and $S_\beta\colon [-\pi, 0] \times \mathbb{R}$ defined by

$$S_q(q) = \bar{S}(-1, q) \quad \text{and} \quad S_\beta(\beta) = \bar{S}\left(\sin(\beta), \cos(\beta)\right).$$

It remains now to define the diffeomorphism ϕ. For that purpose, we propose to construct an ellipse E that best fits $\partial\mathcal{A}$ and a diffeomorphism ϕ that transforms this ellipse into the unit circle. This transformation is affine and can therefore be written as follows:

$$\phi(x) = Ax + b.$$

We denote by $\mathcal{B} = \phi(\mathcal{A})$ the reachable set in the new coordinate system. The proposed transformation is shown in Figure 6.

Since ϕ is an affine transformation, the associated costate transformation is linear (and does not depend on x):

$$p = A^{\top} q.$$

Moreover, thanks to the preservation of the Hamiltonian dynamics by the Mathieu transformation, the geometric interpretation of the costate described in Section 4.1 remains true in the new coordinates.

The shooting function, the reachable set and its polar representation in the new coordinate system are presented in Figures 7, 8 and 9, to be compared to Figures 3, 4 and 5 respectively. As we can see on Figures 8 and 9, the normal cones at the corner points are smaller in the new coordinates. They represent only 15.89% (compare to 99.84% for the original coordinate system) of the angles while the interesting angles (associated to the green part) now represent 42.34% after transformation (compare to 0.066%). Hence, the part of the interesting input set of the shooting function S_β is much bigger than the one for S_α. This is visible on Figure 7.

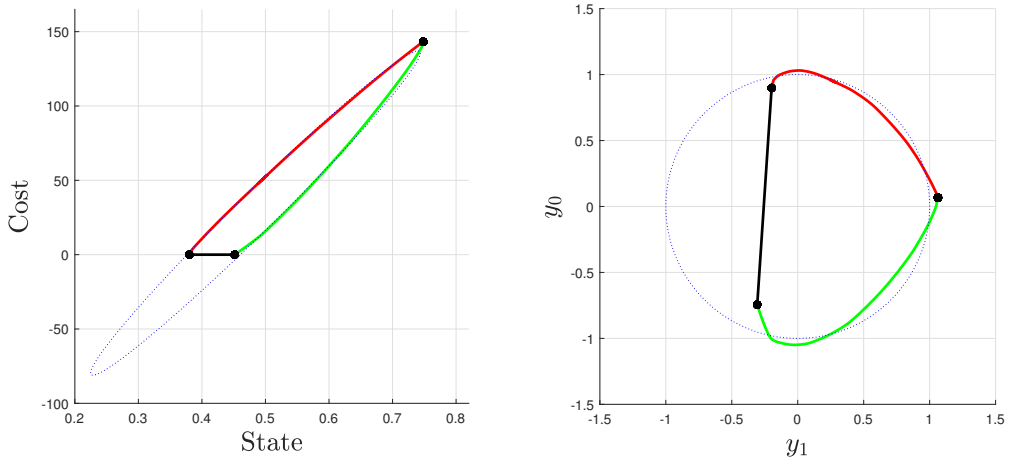

(a) Original coordinate system

(b) New coordinate system

Figure 6: Transformation of the boundary $\partial\mathcal{A}$ of the reachable set in the original coordinate system (6a) into $\partial\mathcal{B}$ in the new one (6b). The fitted ellipse E (dashed blue line on the upper plot) is transformed into the unit circle (dashed blue line on the lower plot).

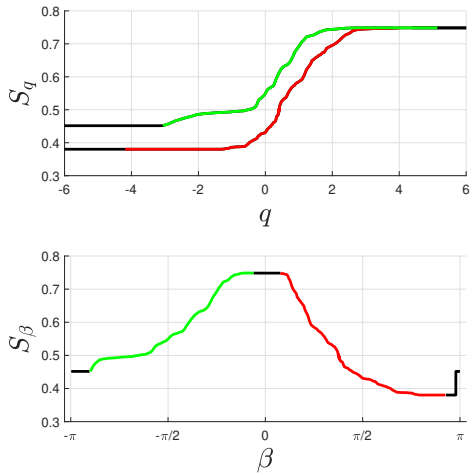

Figure 7: Shooting functions S_q and S_β. To be compared to Figure 3.

5 Results

The goal is now to compare the convergence of the solver with and without preconditioning, for different initial states x_0 and final targets x_f. The convergence of S_p and S_β are compared in two different cases.

In the first case, we suppose that we have no relevant information on what could be a good initial guess, and hence it is arbitrarily fixed to $p = 500$ for S_p and to $\beta = -\pi/2$ for S_β for all the experiments.

The second case is based on [4]. We assume that we have a differentiable approximation $C(x_0, x_f)$ of the value function $V(x_0, x_f)$. This value function corresponds to the optimal cost for Problem (OCP) with the initial x_0 and final x_f state of charge. A method to create such an approximation of the value function is described in [5]. In this context, it has been shown that

$$p_{\text{init}}(x_0, x_f) = \nabla_{x_0} C(x_0, x_f)$$

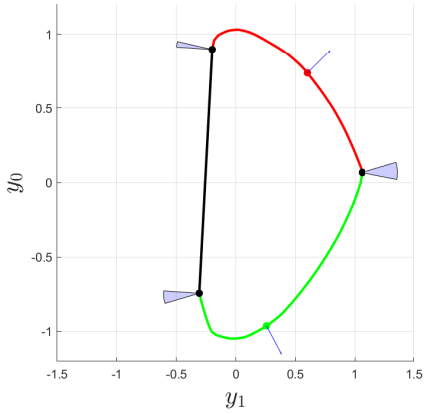

Figure 8: Reachable set in the new coordinate system, where $y = (y_0, y_1)$. To be compared to Figure 4. Notice that the axes now share the same scale.

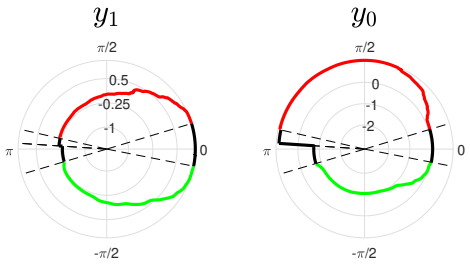

Figure 9: Polar representation in the new coordinate system, where $y = (y_0, y_1)$. To be compared to Figure 5. The black dashed lines correspond to the bounds of the normal cones anchored at the corner points.

is a good initial guess for S_p, and reduces the number of iterations of the solver.

The initial costate $\big(-1, p_{\text{init}}(x_0, x_f)\big)$ is then transported into the q-space and converted in an angle β_{init} by

$$\beta_{\text{init}}(x_0, x_f) = \operatorname{atan2}\left(A^{-\top}\begin{pmatrix} -1 \\ \nabla_{x_0} C(x_0, x_f) \end{pmatrix}\right). \tag{4}$$

Figure 10 shows the evolution of the average error with respect to the number of iterations of the solver. The remarkable fact is that the convergence for the function S_β without the good initial guess (plain orange curve) is faster than the one for the function S_p with the good initial guess (dashed blue curve). Obviously, the best result is clearly obtained when both preconditioner and good initial guess are used (dashed orange curve).

6 Conclusion

In this paper, we propose a new preconditioning method of the shooting function associated to the HEV's torque split and gear shift optimal control problem. This method is based on two main considerations: the geometric interpretation of the costate and the Mathieu transformation. We propose a simple affine application, that transforms an ellipse to the unit circle, and we show that the associated preconditioned shooting function S_β converges faster than the classical one S_p. Moreover, the best result is obtained when a good initial guess (Equation 4) is provided to S_β, thanks to [4].

In a future work, it could be interesting to search for other transformations, possibly non-linear, to reduce even more the number of iterations of the solver. As mentioned previously, the considered cycle is the WLTC on the first 100 seconds. This transformation may be extended to other cycles. It could also be really interesting to study this transformation on general optimal control problems (maybe in higher dimension), and identify which of their properties make it possible to use (or not) this preconditioner.

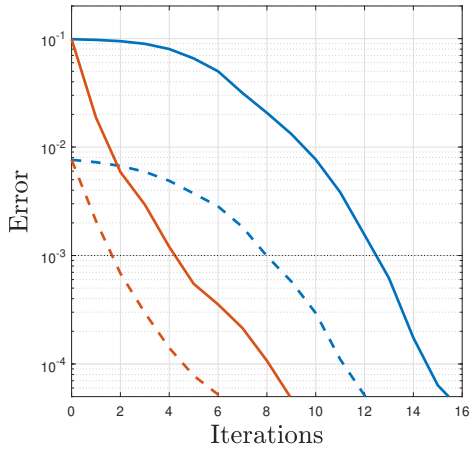

Figure 10: Evolution of the error $|S(\cdot) - x_f|$ with respect to the number of iterations of the solver. The blue curves correspond to the shooting function $S = S_p$ and the orange one to $S = S_\beta$. The plain lines correspond to a fixed initialization ($p = 500$ and $\beta = -\pi/2$), and the dashed ones to the improved initialization ($p = p_{\text{init}}(x_0, x_f)$ and $\beta = \beta_{\text{init}}(x_0, x_f)$). The dotted black line corresponds to the industrial tolerance (10^{-3}).

Acknowledgments

This research was partially supported by Vitesco Technologies. In particular, we want to thank Olivier Flebus, artificial intelligence and optimization group leader at Vitesco Technologies and Mariano Sans, optimal control senior expert at Vitesco Technologies, for their supervision, valuable insights and suggestions.

References

[1] A. A. Agrachev and Y. L. Sachkov, *Control Theory from the Geometric Viewpoint*, Springer Berlin Heidelberg, 2004.

[2] H. Bock and K. Plitt, *A Multiple Shooting Algorithm for Direct Solution of Optimal Control Problems*, IFAC Proc. Vol., 17 (1984), pp. 1603–1608.

[3] L. Cesari, *Statement of the Necessary Condition for Mayer Problems of Optimal Control*, in Optimization—Theory and Applications: Problems with Ordinary Differential Equations, Springer New York, 1983, ch. 4, pp. 159–195.

[4] O. Cots, R. Dutto, S. Jan, and S. Laporte, *A bilevel optimal control method and application to the hybrid electric vehicle*, 2023.

[5] ——, *Generation of value function data for bilevel optimal control method*, 2023.

[6] L. S. Pontryagin, V. G. Boltyanskii, R. V. Gamkrelidze, E. F. Mishechenko, *The Mathematical Theory of Optimal Processes*, Wiley Interscience, New York, 1962.

[7] A. Lesfari, *Géométrie symplectique, calcul des variations et dynamique hamiltonienne*, ISTE Group, 2021.

[8] Y. Saad, *Iterative methods for sparse linear systems*, SIAM, 2003.